Chemistry and Materials Research
ISSN 2224- 3224 (Print) ISSN 2225- 0956 (Online)
Vol.7 No.1, 2015
www.iiste.org

Modelling of Short Corrosion Crack Growth of Low-Alloy Steel in a Chemical environment

Dr. Mahir H. Majeed

University of Middle Euphrates/Technical Institute/Karbala'a PO box 30, Karbalaa, Iraq

Tel: +964 7800 800 608 E-mail: dr.mahir.fte@gmail.com

Abstract

This study aims to develop a theoretical model for short corrosion crack growth rate happen in some of pre-cracked specimens made of three types of low-alloy steel. The selected material is widely used in boiler pipes of electrical power plants. An experimental system was established to simulate the real work conditions, so the specimens subjected to dynamical loading procedure under different chemical environment conditions at different testing temperatures. The results described the behavior of the material under the testing conditions, and showed that the crack growth rate was accelerated due to corrosion contribution, especially at high temperatures, so the classic mechanical crack growth rate under air at room temperature may be neglected as compared with that resulted due to corrosion and temperature interaction. A mathematical model was developed beginning from the superposition model to describe the total crack growth rate of the pre-cracked specimens, depending on many of introduced parameters, such as corrosion density, water chemistry, time of test, crack geometry, loading frequency, stress intensity, velocity of environment liquid motion through the crack walls, and thermal activation energy due to difference in test temperatures. Furthermore, some of important conclusions were outlined.

Keywords: corrosion fatigue crack, crack growth, mathematical model

1. INTRODUCTION

When a metal or an alloy be in contact with an aqueous environment, chemical reactions occurs within the core and on the external surfaces. So if this metal severs from a fatigue load, fatigue/crack growth rate will be influenced by the rates of these reactions depending on the local load concentrations, temperature, and electrode potential that, in turn, depend on mass and charge transfer between the core and the bulk solution.

In many practical instances corrosion may affect crack tip deformation and damage mechanisms, and as a consequence they can modify the crack growth rates as well as the crack path.

There are several studies tried to build a mathematical description for how mass transfers in corrosion fatigue cracks such as George, et al[1], and G. Engelhardt, et al[2], so it was much more complicated than in the corresponding problem under constant load in the case of stress corrosion cracking due to the fluid flow induced by the cyclical displacement of the crack walls. Moreover, it is so difficult to predict whether advection inhibits or enhances the growth of the crack.

Temperature is one of the most important factors in the corrosion cracking of structural materials in a chemical environment, so literatures such as P.M. Scott, et al [3], and S.L. Hong, et al [4] found that the crack growth of nickel-base Alloy 600 and Alloy 182 weld metal in hydrogenated water environments, simulating the pressurized water reactor primary loop coolants, is thermally activated.

In another studies, such as T. Shoji, et al [5], and K. Kumagai, et al [6], microstructural analyses show that most low carbon stainless steels are not thermally sensitized increased hardness or strength by alloy steel has been identified to be crucial for the high crack growth rates.

Stress corrosion cracking can be regarded as the result of localized oxidation enhanced by stress/strain. Here oxidation is a general term representing the process of losing electron from metal, which can be active dissolution of bare metal, or surface film forming/covering, or film thickening.

Low-alloy steels are widely used for many industrial purposes, such as for pressure vessel and reactors piping. The recent research programs, J. Heldt, et al [7] and H.P. Seifert, et al [8] confirmed the relative absence of stress corrosion cracking under static load in of such as pipes in the field, they investigated that a very low susceptibility to crack growth in oxygenated high-temperature water and sustained and fast stress corrosion cracking can only occur under some very specific conditions revealed to the type of chemical environment.

Under the combinations of temperature and strain rate, the component material could eventually reveal higher crack growth rates than the base metal, because of dynamic strain ageing or hydrogen induced environmentally- assisted cracking (if hardness of the material is ≥350 HV) [9].

This investigation aims to satisfy the world-wide demands for higher steam parameters of electrical Power Plants, so there boiling water pipes are made of low alloy steel.

After a brief review on the current status on fatigue crack growth rate for low alloy steel in a chemical environment and by using a crack growth model, the most important environmental, mechanical loading and material parameter trends on cyclic fatigue crack growth are summarized.

Finally, a simple time-domain superposition-model, which could serve as a basis for the development of new improved reference fatigue crack growth rate curves, is outlined.

2. INVESTIGATED MATERIAL

Three different types of low-alloy steels were investigated. Table (1) shows the chemical composition in percentage weight of these types, while Table (2) shows the mechanical tensile test properties of them.

3. EXPERIMENTAL WORK

Corrosion fatigue tests were achieved under simulated environment of boiling piping water of power plants operating conditions. The tests were achieved by fatigue machine which works by completely reversed stress amplitude with zero mean stress. A revolution counter was fitted to the machine motor to record number of cycles when specimen is fractured. Rode air fatigue pre-cracked specimens were prepared from the three types of the investigated alloys with a geometry and method that described by Hussain, et al [11]. Two specimens are used for each test to accurate the results.

The specimen loaded inside a stainless steel autoclaves container that allows a chemical water to flow through it after shooting the specimen. The heated chemical water is injected by a piping system integrated with a pump, and a multi-heater boiler which can keep the chemical water with a required temperature through the tests. The testing system is shown in Figure (1).

To simulate the operating conditions, additional tests at temperatures of 100, 175, and 288 ^{o}C were performed as well as sulphate or chloride in terms of H_2SO_4 or HCl, respectively, were added separately to the high-purity water in the experiments. During the experiments, all important data were recorded continuously. The reversed direct current potential drop method (DCPD) with a resolution limit of about 2–5 µm used to monitor the crack advance continuously.

4. RESULTS AND DISCUSSION

The experimental tests yielded many of results. Such results indicated the behavior of the investigated material when it loaded under the chemical environment or without it. This behavior affected by the environment conditions and the temperature of test. Here, some of these results will be shown by curves and discussed by phenomena. Not all of the results are mentioned in this paper, only those which can give a clear indication about what happen for the investigated material through the test until failure. Furthermore, this study does not responsible of the physical mean or the scientific reasons of the material failure due to corrosion fatigue crack growth, but it deals with how this growth can be modeled mathematically under work conditions similar to those that subjected experimentally to the investigated material. Thus, the experimental results will be partly explained and discussed only for achieving the main goal of this study.

The results show the advantage of using specimens under various test conditions with continuous monitoring to investigate the crack growth mechanism.

First of all, the classic *stress-no. of cycles to failure* curve can give a whole picture of the failure behavior of the investigated material due to air crack growth as compared with its failure due to corrosion crack growth due to applying hot pure water at different temperatures. Fig. (2) shows this comparison for SA1 alloy type, so it indicates that the main effect which accelerate the failure is the corrosion contribution due to chemical environment at high temperature.

Relevant environmental effects on fatigue life and short crack growth were typically observed above 100 and 175 ^{0}C, respectively. Above this threshold the environmental reduction of fatigue life and acceleration of fatigue crack growth increased with increasing temperature and were more pronounced than in air, where temperature usually has little effect on fatigue life between 25 and 100 ^{0}C.

The blue solid line in Fig.(2) shows high dangerous of fast failure of the material as compared with its failure under air at room temperature condition presented by the dashed line. This result was repeated for other investigated alloys, SA2 and SA3, and agreed with the results of some of past studies such as Ref.[12]. The main reason of that is the clear contribution of the corrosion effect in accelerating the crack growth rate due to the environmental condition of water and temperature.

The three types of the selected alloys, SA1, SA2, and SA3, show the similar behavior at the highest temperature of test, 288 ^{0}C, which is the most dangerous temperature on the material life under corrosion condition. So Fig. (3) explains this result.

The very small differences in fatigue life between the three investigated alloys is for the very differences between the chemical compositions and mechanical properties of them as presented in Tables (1) and (2) above. This similarity is agreed with that presented by Refs. [13, 14], while Ref. [15] concluded that the environmental reduction of fatigue life and environmental acceleration of the stationary short fatigue crack growth was comparable for the low-carbon (304L and 316L) and the stabilized grades (321 and 347) as well as for sensitized and solution annealed stainless steels. A similar behavior was also observed in tests with long cracks by Ref.[16].

Besides the effect of material strength on the crack tip mechanics, such as the stress/ strain distribution and strain rate at the crack tip, increasing the strength of a material by hardening generally increases the internal energy of the materials, especially the grain boundary energy by the accumulation of dislocations, which might also have an effect on the corrosion kinetics, the resultant crack growth rate and the apparent activation energy [17].

Now, by depending that the fatigue life under test temperature of 288 ^{0}C is the most affected for the three selected alloys, it is important to know the difference between the effect of added chemical components to the water with the effect of pure water for the same temperature, 288 ^{0}C. Fig. (4) shows the required difference for the investigated alloy SA3, so the showed result is closed similar to those for the other alloys, SA1 and SA2.

Fig. (4) shows that the chemical water reduces the fatigue life of the material as compared with pure water at the same temperature. That means the corrosion contribution in crack growth rate be greater due to what components added to the pure water. This phenomena is agreed with what resulted by [13, 14].

The corrosion fatigue life results drive the study to focus on the crack growth rate rather than fatigue life, because it is the main reason of failure of the pre-cracked specimens. The average crack length, a, was calculated by averaging more than 40 measurements at different positions, which is the method used for converting the (DCPD) signal to crack length, among the test time, t. so the crack growth rate (d_a/d_t) can be known. Fig. (5) shows the relationship between the crack growth rate with a corrosion contribution at 288 ^{0}C and that under air condition at room temperature. It is enough here to show this relation only after it be known that the failure is accelerated by chemical water, so it is the most important parameter to be compared with the usually case of fatigue failure under air condition at room temperature which there is no corrosion could be happen.

It is noted that by Fig. (5), the corrosion crack growth rate is most larger than the crack growth rate under air without corrosion contribution, so the $(d_a/d_t)_{air}$ may be neglected in the calculation of the total crack growth rate which achieves the failure, so this result is agreed with Ref.[1].

As it was sensed, crack length does not increase linearly with time, so a mathematical model must be developed for determining the crack growth rate is important in order to obtain the relevant crack growth rate data and for further quantitative analysis of the influential factors.

Another notice was obtained, that is the effect of yield strength would be complex because of the potential effect of yield strength on the chemical environment. High yield strength would enhance the crack tip corrosion within localized crack tip area due to highly localized stress and strain. It implies that the reaction rate could be significantly affected by the crack tip stress, which would be the contents of future work. The theoretical crack tip asymptotic filed needs to be more precisely confirmed or determined by numerical simulations or other approaches. The present analysis is mainly focusing on modeling of crack growth rate under constant chemical environment conditions.

The temperature may relevantly vary in the real field of work depending on component location in a range of (274–288 ^{0}C), so it was clear that the crack growth rate does not affected by corrosion contribution only, the increasing temperature of pure and chemical water affects mainly in increasing the rate of crack growth. This result can be shown by Fig. (6). This fact agrees with many of past studies such as [11, 12, 13, 17].

Fig. (6) shows that the crack growth rate increases monotonically with increasing temperature after 175 ^{0}C. The general trend of this dependence is similar in both cases of pure water or chemical water environment, confirming that the crack growth is thermally activated after this temperature.

The temperature is a parameter that universally affects all the physical and chemical processes. Temperature can affect stress corrosion cracking through its effect on the material, mechanical, and environmental properties, and their interactions. Material parameters such as the yield and tensile strength decrease with increasing temperature [17]. The thermodynamic properties of the water chemistry are also strongly dependent on the temperature. In the temperature range from 0 to 200 ^{0}C, the water conductivity and water dissociation constant increase significantly with increasing temperature, while the pH decreases with increasing temperature [18]. The differences between the temperature dependencies of the crack growth rate and these water properties imply that the difference in the thermodynamic properties of bulk water may not be the primary cause for the thermally activated stress corrosion cracking growth.

Ref. [19] reported a similar case of thermally activated crack growth behavior for sensitized 304SS in oxygenated pure water. The differences in the temperature dependencies of the crack growth rate are thought to be due to differences in water chemistry, such as the dissolved oxygen content and added chemicals, test methods and loading patterns. As described by Ref. [20], the apparent activation energy for the crack growth rate reflects the overall effects of temperature on the elementary processes involved in crack growth, which is different from the concept for homogeneous reactions. The apparent activation energies for the crack growth rates can thus be affected by materials properties and experimental parameters that may change the ratio of the contribution from each elemental reaction.

5. MATHEMATICAL MODEL

Since there are still some uncertainties in selecting input parameters in the theoretical crack growth rate equations, the set of input parameters used in modeling is subjected to modification as more exact experimental data (such as oxidation kinetic laws especially at grain boundaries under stress and other input parameters) become available [21].

In the following paragraphs, a superposition- model for the evolution of engineering reference fatigue crack growth curves in high-temperature chemical water is outlined, which is based on the time-domain analysis and some of the most dominant experimental parameter effects, but ignores material aspects in the present form[22].

Accordance to superposition model [23], it is assumed that the corrosion fatigue crack growth rate, $\left(\frac{da}{dt}\right)_{tot.}$, can be presented in the form:

$$\left(\frac{da}{dt}\right)_{tot.} = \left(\frac{da}{dt}\right)_{air} + \left(\frac{da}{dt}\right)_{en.} \quad \text{.....(1)}$$

Where; $\left(\frac{da}{dt}\right)_{air}$ is pure mechanical fatigue crack growth rate at air, and;

$\left(\frac{da}{dt}\right)_{en.}$ is the environmentally contribution.

Under cyclic loading conditions, it is assumed that the crack tip strain rate is proportional to the experimentally derived and known fatigue crack growth rate in air ($d\varepsilon/dt \; \alpha \; da/dt_{air}$) under otherwise identical loading conditions.

In this investigation, it considered that only the case when the environmental component, $\left(\frac{da}{dt}\right)_{en.}$, is caused by the anodic dissolution of the alloy matrix at the crack tip, and due to the Faraday's law, $\left(\frac{da}{dt}\right)_{en.}$ is proportional to corrosion current density, i, as following[17]:

$$\left(\frac{da}{dt}\right)_{en.} = \left(\frac{M}{\rho z F}\right).\left(\frac{i(t)}{t}\right) \quad \text{.....(2)}$$

where; M is the molecular weight, F is Faraday's constant, z is the oxidation valiancy, and ρ is the density.

These factors depend on the characteristics of the used material and chemical environment.

As shown in Fig.(7), it is considered that the metal is dissolved at the tip of the long parallel slot with pulsating walls, so the current density at the crack tip is given by [1] as following:

$$i = -zFD\left(\frac{\partial C}{\partial x}\right)_{x=0} \quad \text{.....(3)}$$

where: D is the diffusion coefficient, and C is the concentration of species.

By considering that C varies from bulk concentration, C_0, to saturation state, at surface concentration, C_s, Eqn. (3) can yield:

$$i = zF\beta\frac{C_s - C_0}{Lg_{\min}}g(t) \quad \text{.....(4)}$$

where: L is the horizontal length of the crack as shown in Fig. (7), and $g(t)$ is an arbitrary function of time, and for a period of oscillation, τ>0:

$$\frac{1}{\tau}\int_0^{\tau} g(t)dt = 1 \quad \text{.....(5)}$$

So the minimum and maximum values of the function $g(t)$, respectively, are:

$$0 < g_{\min} \le 1, \text{ and; } 1 \le g_{\max} < \infty \quad \text{.....(6)}$$

Therefore, the Average current density, i_{av}, over the period of oscillation, τ, will be:

$$i_{av.} = \frac{1}{\tau}\int_0^{\tau} i dt = zFD\frac{C_s - C_0}{Lg_{\min}} \quad \text{.....(7)}$$

If the new variable, y, is introduced as:

$$y = xg(t) \quad \text{.....(8)}$$

Therefore, the boundary conditions will be:

$$\text{when } y = 0,\ C = C_s \text{ , and; when } y = Lg_{\min},\ C = C_0$$

For numerical calculations, the case of sinusoidal movement of walls were performed at C_0 = 0.01 M, and C_s = 1 M, so the relationship between C and y for the whole period of test can be expressed by Fig.(8) as concluded by Ref.[1].

The limiting diffusion current density, i_d, can be calculated in the absence of convection, for a stress corrosion crack, by the factor:

$$\frac{i_{av.}}{i_d} = \frac{1}{g_{\min}} \quad \text{.....(9)}$$

This causes an increase in corrosion rate.

So that for known crack length L, the parameter y will be known, corresponding to known C by referring to Fig.(8), then g_{min} will also be known by determining it by Eqn.(8) and its boundary conditions. Thus, the factor ($i_{av.}/i_d$) will be calculated.

The sinusoidal wall movement can be described corresponding to the arbitrary function, $g(t)$, by the following equation:

$$g(t) = 1 + \varepsilon \sin(\omega t) \quad \text{.....(10)}$$

Where; ω is the cyclic loading angular frequency (f), and it can be known by:

$$\omega = 2\pi f \quad \text{.....(11)}$$

The constant ε is a known constant, and its value is less than one. So ε, and the dimensionless frequency, f^*, affect the dimensionless factor ($i_{av.}/i_d$) by considering the following function, ϕ:

$$\Phi(\varepsilon, f^*) = \frac{(i_{av.}/i_d) - 1}{(1/g_{\min}) - 1} \quad \text{.....(12)}$$

The behavior of this function can be displayed by Fig.(9) for two curves, at ε = 0.25 (solid line) and ε=0.75 (dashed line)[1], so the dimensionless frequency, f^*, can be estimated.

The dimensionless frequency, f^*, is proportional to the diffusion coefficient, D, as following:

$$f^* = \frac{fL^2}{D} \quad \text{.....(13)}$$

where; f is the known frequency due to the loading procedure. So, D, will be known.

The averaged corrosion current density, $i_{av.}$, over the period of oscillation as, a function of loading frequency, f, is expressed by Fig.(10), for different values of ε.

It is seen that advection increases the corrosion current density, when the crack growth rate is diffusion controlled, but advection primarily reduces the corrosion current density in the case of mixed kinetics. The explanation is that advection decreases the concentration of the electrolyte near the crack mouth and, in doing so, increases the resistance (and, hence, the potential drop) of the solution down the crack[1]. This fact can be important from the point of view of analyzing experimental data.

Therefore, and due to the experimental results, $\left(\frac{da}{dt}\right)_{en.} >> \left(\frac{da}{dt}\right)_{air}$, so that, by referring to Eqn.(1), it can be considered that $\left(\frac{da}{dt}\right)_{tot.}$ is approximately equal to $\left(\frac{da}{dt}\right)_{en.}$, so that agrees with Ref.[1]. In this case, the maximum value of $\left(\frac{da}{dt}\right)_{en.}$ can be calculated by Eqn. (2) when the corrosion current density, i, is considered as the limiting diffusion current density, i_d, when saturation at the crack tip is reached.

Now, as a comparison with the experimental results, if the experimentally measured value of $\left(\frac{da}{dt}\right)_{tot.}$ is greater than, or equal to, that derived from this theoretical model, it means that corrosion fatigue takes place

under diffusion control. On the other hand, if $\left(\frac{da}{dt}\right)_{tot.}$ is greater than the theoretically determined by a factor of ($1/g_{min}$), it means that crack propagation rate is not determined by anodic dissolution.

The environmental effect factor, $F_{en.}$, can be defined for test results for the environmental reduction as an acceleration of the subsequent stationary short crack growth by the following equation[12]:

$$F_{en.} = \frac{\left(da/dt\right)_{en.}}{\left(da/dt\right)_{air}} \text{.....(14)}$$

Referring to Fig.(7), metal is dissolved at the tip of the slot with pulsating walls moving in accordance with the equation:

$$w(t) = w_{av.} g(t) \text{.....(15)}$$

where; w is the width of the pulsating wall crack, and $w_{av.}$ is the average width of the crack over the period of oscillation, so it presents the mean value of $w(t)$ over the period of oscillation.

It is easy to analyze the trapezoidal geometry of the crack by introducing the equivalent parallel-sided crack whose width is equal to the average crack width of the trapezoid [24]. The width of trapezoid crack can be described by the following equation [25]:

$$w(x,t) = D_{tip}(t) + x\frac{D_{op}(t) - D_{tip}(t)}{2a} \text{.....(16)}$$

where; D_{tip} is the crack tip displacement, D_{op} is the crack opening displacement at the loading line, and a is the crack length from the cavity tip to the loading line.

Then the equivalent width of the parallel-sided crack can be formulated as:

$$w(t) = \frac{1}{L}\int_0^L w(x,t)dx = D_{tip}(t) + L\frac{D_{op}(t) - D_{tip}(t)}{4a} \text{.....(17)}$$

As adopted in Ref. [24], Eqn.(17) describes the average width of a sufficiently deep crack with a length larger than (2 mm), thus, when $D_{op} >> D_{tip}$, and $(LD_{op}/4a) >> D_{tip}$, $w(t)$ will be proportional to D_{op} as ($w(t) \approx \frac{LD_{op}}{4a}$)

The parameter D_{op} is proportional to the stress intensity factor $K(t)$ [26]. The stress intensity factor, $K(t)$, varies with time if the loading is assumed to be sinusoidal for numerical simulations [24], so it can be calculated as following:

$$K(t) = K_{av.} + \frac{1}{2}\Delta K \sin(\omega t) \text{.....(18)}$$

where; $K_{av.}$ is the averaged stress intensity factor, and it depends on the experimental loading procedure. Therefore;

$$\varepsilon = \frac{\Delta K}{2K_{av.}} \text{.....(19)}$$

where; ΔK is the stress intensity factor range of fatigue cycle, and it is proportional to D_{op} by the following relationship [12]:

$$\Delta K = \frac{4\Delta P \psi(D_{op}/W)}{\pi d^2/\sqrt{W}} \text{.....(20)}$$

where; ΔP is load range of fatigue cycle, known experimentally, $\psi(D_{op}/W)$ is a function calculated according to ASTM E399[27], and d and W are the diameter and length of the specimen, respectively, known by specimen geometry.

So that D_{op} will be known, then, by Eqs.(17) and (15), $w(t)$ and $w_{av.}$, respectively, will be known, too.

The movement velocity, v, of the environment liquid within the crack can be found from the equation of continuity in the one dimensional approximation as:

$$\frac{\partial w}{\partial t} + \frac{\partial vw}{\partial x} = 0 \text{.....(21)}$$

For an approximately parallel slot, the velocity of the fluid within the crack can be rewritten as:

$$v(x,t) = -\frac{1}{w(t)}\int_0^x \frac{\partial w}{\partial t}dx = -\frac{g'(t)}{g(t)}x \quad \text{.....(22)}$$

The effect of temperature on the crack growth rate for any two temperatures can be noted by using Eqn.(23) under condition of measuring the steady crack growth rates for each temperature under constant dissolved oxygen conditions rather than maintaining a constant chemical potential[17].

$$E_{\Delta T} = \frac{T_1 T_2}{T_2 - T_1}\ln\frac{(da/dt)_{T_2}}{(da/dt)_{T_1}} \quad \text{.....(23)}$$

where; $E_{\Delta T}$ is thermal activation energy on the crack growth rate due to the difference in the test temperature.

It may not have been possible to have kept the chemical potential at the crack tip constant at different temperatures even though the bulk chemical potential could have been fixed at the same value at different temperatures by adjusting the dissolved oxygen content.

The apparent activation energy is expected to be constant if the crack growth rate is controlled by a single process in a certain temperature range.

This developed theoretical model can be applied, not only for the case of metal corrosion in the solution of its own salt, as has been done for simplicity in this investigation, but also to the case of an arbitrary number of chemical reactions that take place at the tip of the crack and for any arbitrary number of chemical reactions that take place inside the crack.

Computer codes for performing the calculations of such models can be reviewed in Refs.[28, 29, 30]. This developed models and codes are possible to be used for estimating stress corrosion crack growth rate for also estimated corrosion fatigue crack propagation rate. Such numerical experiments may be done for future work.

6. SUMMARY AND CONCLUSIONS

Many of pre-cracked specimens of three types of low-alloy steel material were tested by fatigue loading under chemical environment and different temperature conditions. A mathematical model was developed to describe the corrosion crack growth rate due to these tests. Many of parameters were included in this model. The following conclusions were resulted:

1. By particular testing and monitoring, the corrosion contribution, and temperature parameters and their potential variation seem to be the most important factors that influencing corrosion crack growth rate, while material parameters played a less pronounced role in this investigation.

2. The developed mathematical model seems to be reasonably well predicting the experimentally observed parameter trends that affect the corrosion crack growth rate. It could reduce most of the undue conservatism and eliminate uncertainties of the existing codes, so it can serve as a basis for the development of improved reference fatigue crack growth curves for future work.

3. There is no good chance that the current investigated material could be used for the water boiler pipes in the power plants under conditions of water chemistry because it couldn't cover the corrosion fatigue crack growth in studied environment conditions.

4. The applied experimental technique with pre-cracked specimens allowed the study of environmental effects on physical fatigue short crack growth separately. The separation encourages the elimination of some apparent discrepancies between different lab investigations and to avoid certain misconceptions.

5. The behavior of all types of the investigated material, either under pure water or chemical water conditions, is similar, especially at high test temperature.

6. For future work, and to improve the accuracy the mathematical model, more fundamental data for oxidation kinetic laws and crack tip mechanics are necessary to input parameters in the crack growth rate equations. So that damage mechanism taking place during crack growth should be taken into account by applying advanced models for fatigue crack propagation.

7. The temperature-dependent activation energy can be explained by taking into consideration the effects of temperature on the multiple element processes involved in the crack tip corrosion kinetics.

References

1. George R. Engelhardt a, Digby D. Macdonald; Modelling the crack propagation rate for corrosion fatigue at high frequency of applied stress; Corrosion Science 52 (2010) 1115–1122.

2. G. Engelhardt, D.D. Macdonald; Modeling of Corrosion Fatigue Crack Propagation; Corrosion'2001, NACE International, Houston, TX, 2001.

3. P.M. Scott, C. Benhamou, An overview of recent observation and interpretations of IGSCC in nickel base alloys in PWR primary water, in: Proceedings of the 10th International Symposium on Environmental Degradation of Materials in Nuclear Power Systems–Water Reactors, NACE, 2001, CDROM.

4. S.L. Hong, J.M. Boursier, C. Amzallag, J. Daret, Measurement of stress corrosion growth rates in weld alloy 182 in primary water, in: Proceedings of the 10th International Symposium on Environmental Degradation of Materials in Nuclear Power Systems–Water Reactors, 2001, NACE, CD-ROM.

5. T. Shoji, Progress in the mechanistic understanding of BWR SCC and its implication to the prediction of SCC growth behavior in plants, in: Proc. 11th Int. Symposium. Environ. Degradation of Materials in Nuclear Power Systems-Water Reactors, ANS, 2003, p. 588.

6. K. Kumagai, S. Suzuki, J. Mizutani, C. Shitara, K. Yonekura, M. Masuda, T. Futami, Evaluation of IGSCC growth behavior of 316NG PLR piping in BWR, in: Y.Y. Wang (Ed.), Residual Stress, Fracture, and Stress Corrosion Cracking, PVP-vol. 479, ASME, 2004, p. 217.

7. J. Heldt, H.P. Seifert, Nuclear Engineering and Design 206 (2001) 57–89.

8. H.P. Seifert, S. Ritter, Journal of Nuclear Materials 372 (2008) 114–131.

9. H.P. Seifert, S. Ritter, Research and service experience with environmentally assisted cracking of carbon and low-alloy steels in high-temperature water, SKI-Report 2005:60, Stockholm, Sweden, 2006.

10. H.P. Seifert, S. Ritter, U. Ineichen, U. Tschanz, B. Gerodetti, Risskorrosion in druckführenden Komponenten des Primarkreislaufes von SWR, PSI Report 03-10, PSI, Switzerland, April 2003.

11. Hussain J. Al-alkawi, Dhafir S. Al-Fattal, and Mahir H. Majeed, Effect of Hold Time Periods at High Temperature on Fatigue Life in Aluminum Alloy 2024 T4, Engineering & Technology Journal, 2010 Volume: 28 Issue: 2608-2621, University of Technology.

12. H.P. Seifert, S. Ritter, H.J. Leber, Corrosion fatigue initiation and short crack growth behavior of austenitic stainless steels under light water reactor conditions, Corrosion Science 59 (2012) 20–34.

13. H.P. Seifert, S. Ritter, Corrosion fatigue crack growth behavior of low-alloy reactor pressure vessel steels under boiling water reactor conditions, Corrosion Science 50 (2008) 1884–1899.

14. S. Ritter, H.P. Seifert, Effect of corrosion potential on the corrosion fatigue crack growth behavior of low-alloy steels in high-temperature water, Journal of Nuclear Materials 375 (2008) 72–79.

15. H.P. Seifert, S. Ritter, Environmentally-Assisted Cracking in Austenitic Light Water Reactor Structural Materials – Final Report of the KORA-I Project, PSI Report No. 09–03, Paul Scherrer Institute, Villigen PSI, Switzerland, 2009.

16. H.P. Seifert, S. Ritter, H.J. Leber, Corrosion fatigue crack growth behaviour of austenitic stainless steels under light water reactor conditions, Corrosion Science 55 (2012) 61–75.

17. Zhanpeng Lu , Tetsuo Shoji, Yoichi Takeda, Yuzuru Ito, Seiya Yamazaki, The dependency of the crack growth rate on the loading patternand temperature in stress corrosion cracking of strain-hardened 316L stainless steels in a simulated BWR environment, Corrosion Science 50 (2008) 698–712.

18. M. Vankeerberghen, D.D. Macdonald, Corros. Sci. 44 (7) (2002) 1425–1441.

19. A. Jenssen, C. Janson, Effects of temperature on crack growth rate in sensitized type 304 stainless steel in pure and sulfate bearing BWR environments, in: Proceedings of the 10th International Symposium on Environmental Degradation of Mater. Nuclear Power Systems– Water Reactors, NACE, 2001, CDROM.

20. G. Santarini, Corrosion 51 (9) (1995) 698–710.

21. Tetsuo Shoji, Zhanpeng Lu , Hiroyoshi Murakami, Formulating stress corrosion cracking growth rates by combination of crack tip mechanics and crack tip oxidation kinetics, Corrosion Science 52 (2010) 769–779.

22. H.P. Seifert, S. Ritter, Research and service experience with environmentally-assisted cracking in carbon and low-alloy steels in high temperature water, SKI-Report 2005:60, Villigen, Switzerland, 2005.

23. R.P. Gangloff, Environment Induced Cracking of Metals, NACE, Houston, 1990. pp. 55–109.

24. A. Turnbull, Corros. Sci. 22 (1982) 877.

25. A. Turnbull, D.H. Ferris, Corros. Sci. 27 (1987) 1323.

26. A. Saxena, S.J. Hudk, Int. J. Fract. 14 (1978) 453.

27. Active Standard ASTM E399, Standard Test Method for Linear-Elastic Plane-Strain Fracture Toughness KIc of Metallic Materials, Developed by Subcommittee: E08.07, Book of Standards Volume: 03.01.

28. G. Engelhardt, M. Urquidi-Macdonald, D.D. Macdonald, Corros. Sci.39 (1997) 419.

29. S.M. Sharland, Corros. Sci 27 (1987) 289.

30. A. Turnbull, Br. Corros. J. 28 (1993) 297.

Table (1): Chemical composition in wt.% of investigated steels [10]

Material	**Alloy code**	**C**	**Si**	**Mn**	**P**	**S**	**Cr**	**Mo**	**Ni**	**V**	**Al**	**cu**	**Fe**
SA 533 B Cl.1	SA1	0.25	0.24	1.42	0.006	0.018	0.12	0.54	0.62	0.007	0.03	0.15	Rest.
SA 508 Cl.2	SA2	0.21	0.27	0.69	0.005	0.004	0.38	0.63	0.78	0.006	0.015	0.16	Rest.
SA 508 Cl.3	SA3	0.21	0.25	1.26	0.004	0.004	0.15	0.5	0.77	0.008	0.013	0.06	Rest.

Table (2): Mechanical tensile test properties of investigated steels [10]

Alloy code	**T=25 ^{o}C**				**T=100 ^{o}C**	**T=175 ^{o}C**	**T=288 ^{o}C**
	σ_y (MPa)	**σ_u (MPa)**	**Elongation %**	**reduction of area %**	**σ_y (MPa)**	**σ_y (MPa)**	**σ_y (MPa)**
SA1	456	605	23.4	59.9	439	428	412
SA2	448	611	17.9	71.0	433	418	396
SA3	485	648	19.3	72.1	466	447	418

where; T is test temperature, σ_y is yield stress, and σ_u is ultimate strength.

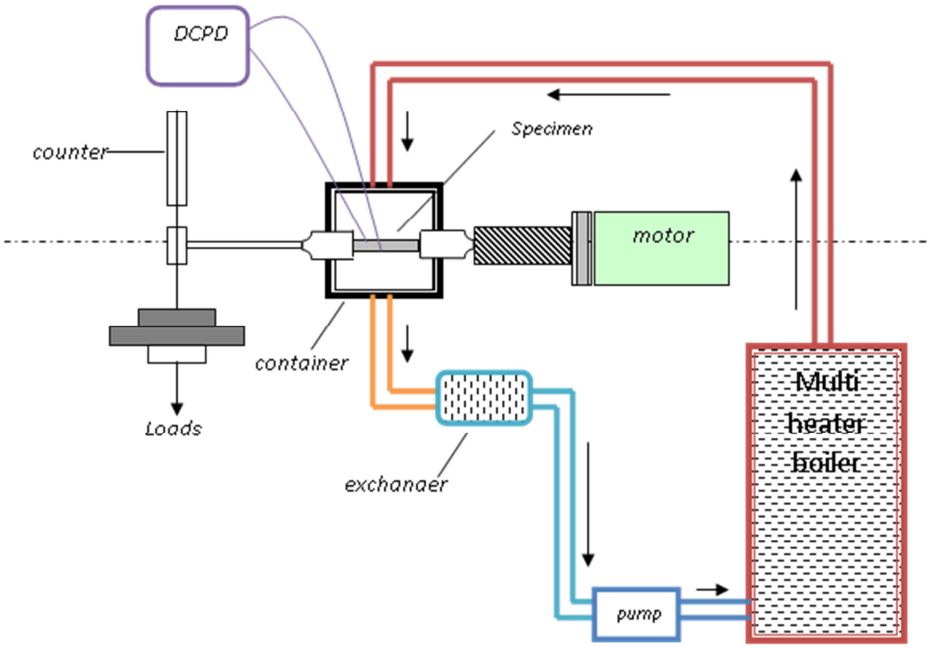

Figure (1): corrosion fatigue testing system

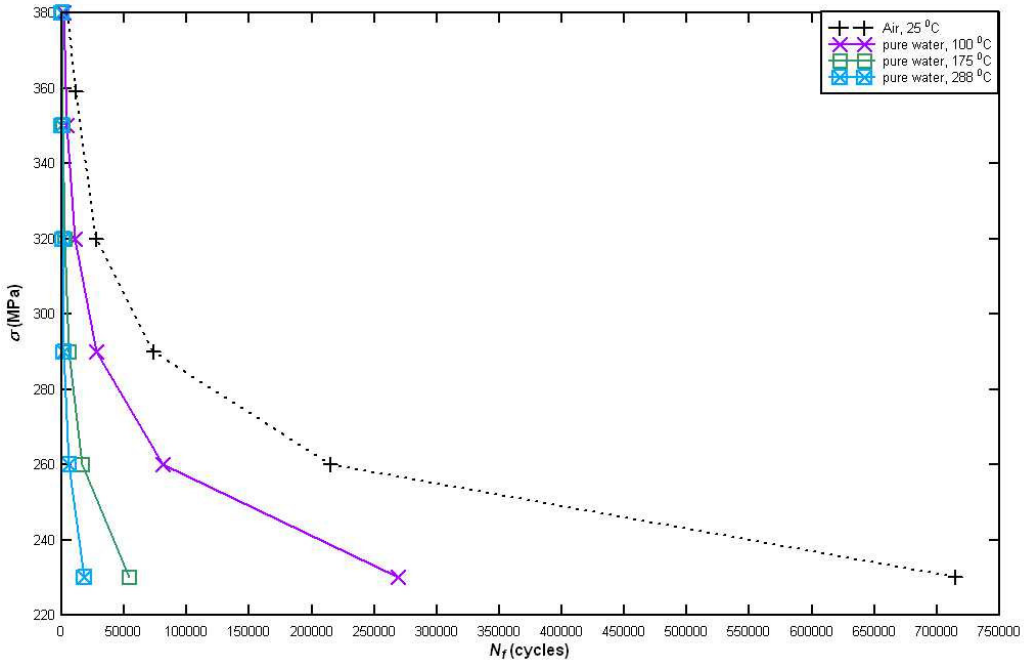

Fig. (2); stress, σ, versus no. of cycles to failure, N_f curve for SA1 alloy under air at room temperature and pure water at different high temperatures.

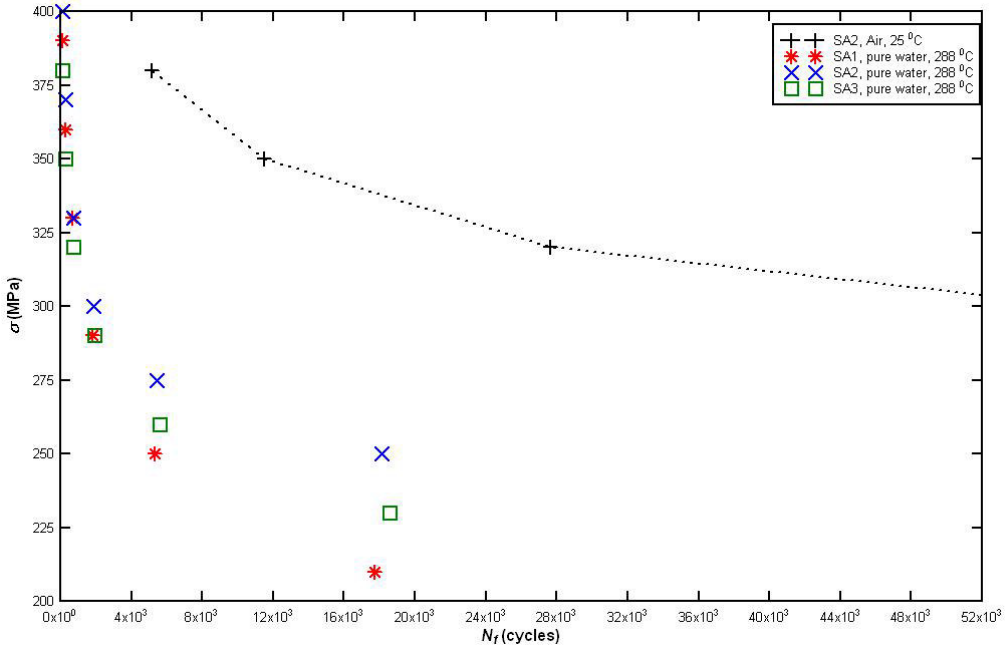

Fig. (3); stress, σ, versus no. of cycles to failure, N_f curve for SA1, SA2, and SA3 alloys under pure water at 288 ^{0}C as compared with that for SA2 under air at room temperature.

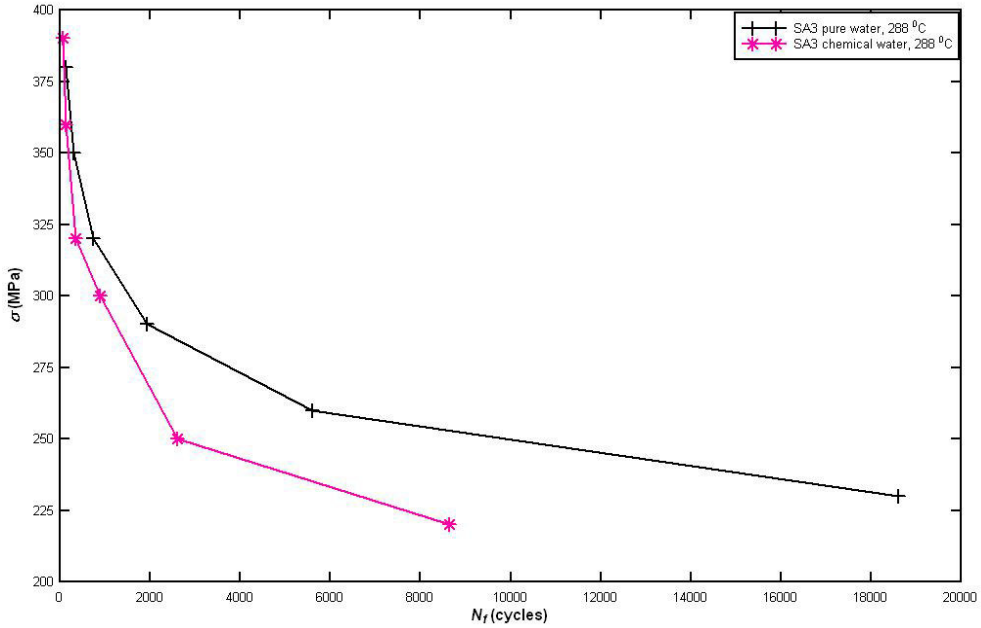

Fig. (4); stress, σ, versus no. of cycles to failure, N_f curve for SA3 alloy under pure water and chemical water at 288 ^{0}C.

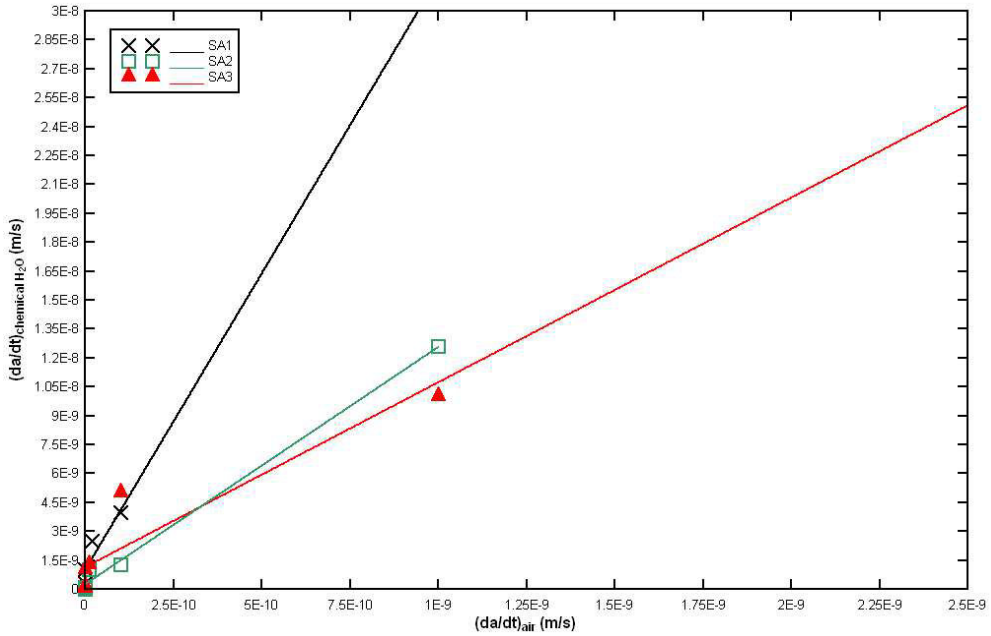

Fig. (5); corrosion crack growth rate as a function of that of air for the three investigated alloys, SA1, SA2, and SA3 at 288 ^{0}C.

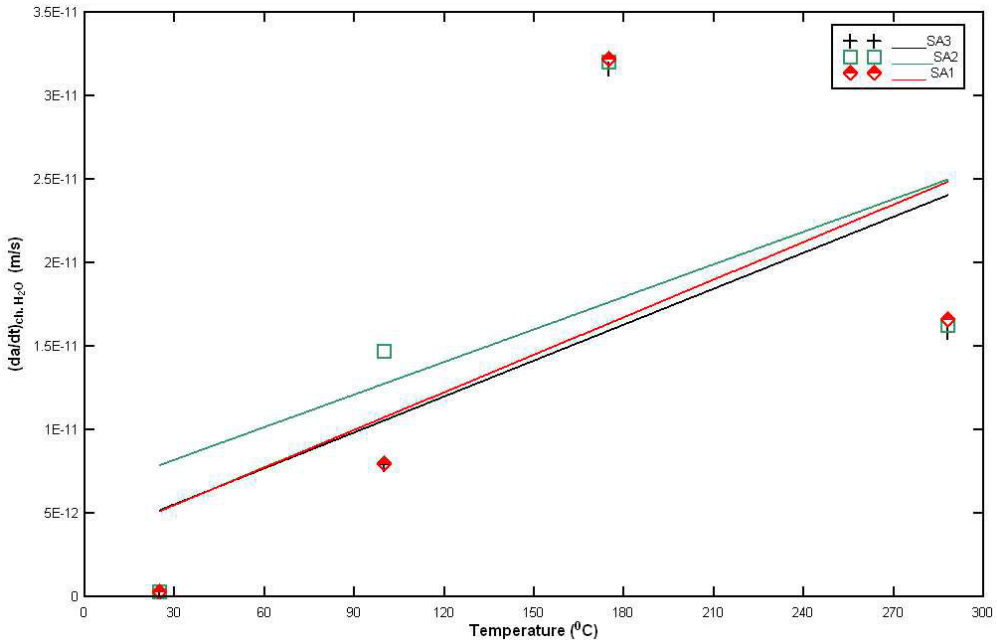

Fig. (6); the relationship between the corrosion crack growth rate and temperature for the three investigated alloys, SA1, SA2, and SA3.

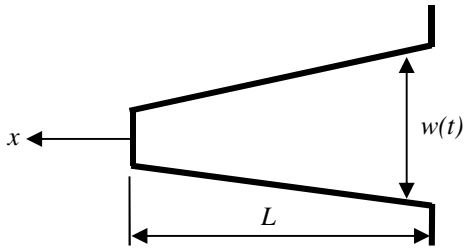

Fig. (7); assumed crack geometry

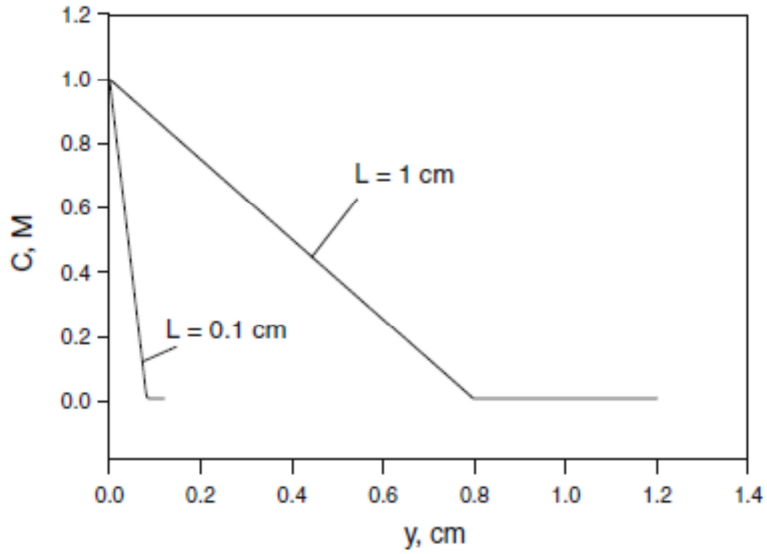

Fig. (8); steady-state concentration of the corroding metal under diffusion control as a function of parameter *y* for different lengths of the corroding crack.

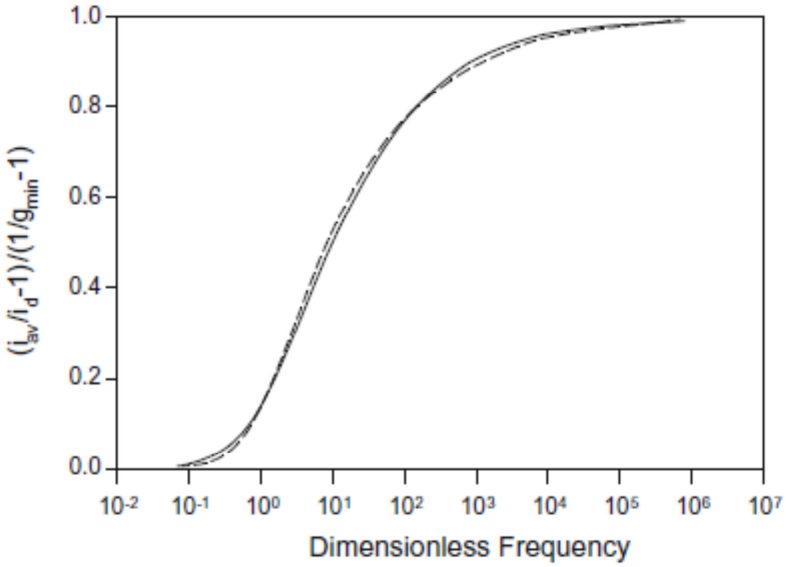

Fig. (9); description of function ϕ

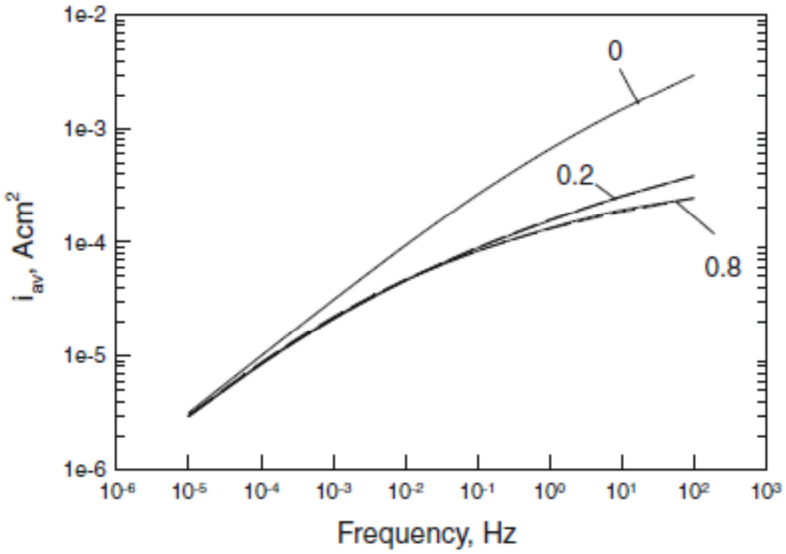

Fig.(10); averaged corrosion current density as a function of loading frequency at different values of ε.

The IISTE is a pioneer in the Open-Access hosting service and academic event management. The aim of the firm is Accelerating Global Knowledge Sharing.

More information about the firm can be found on the homepage:
http://www.iiste.org

CALL FOR JOURNAL PAPERS

There are more than 30 peer-reviewed academic journals hosted under the hosting platform.

Prospective authors of journals can find the submission instruction on the following page: http://www.iiste.org/journals/ All the journals articles are available online to the readers all over the world without financial, legal, or technical barriers other than those inseparable from gaining access to the internet itself. Paper version of the journals is also available upon request of readers and authors.

MORE RESOURCES

Book publication information: http://www.iiste.org/book/

Academic conference: http://www.iiste.org/conference/upcoming-conferences-call-for-paper/

IISTE Knowledge Sharing Partners

EBSCO, Index Copernicus, Ulrich's Periodicals Directory, JournalTOCS, PKP Open Archives Harvester, Bielefeld Academic Search Engine, Elektronische Zeitschriftenbibliothek EZB, Open J-Gate, OCLC WorldCat, Universe Digtial Library , NewJour, Google Scholar